Lignin-Based Carbon/$CePO_4$ Nanocomposites: Solvothermal Fabrication, Characterization, Thermal Stability, and Luminescence

Shu-Ming Li,[a] Shao-Long Sun,[a] Ming-Guo Ma,[a,*] Yan-Yan Dong,[a] Lian-Hua Fu,[a] Run-Cang Sun,[a,b] and Feng Xu [a]

This work explored the synthesis of carbon-based luminescent materials using cheap, natural resources. Lignin-based carbon/$CePO_4$ nanocomposites were successfully synthesized using previously extracted lignin solution and $CePO_4$, or NaH_2PO_4•$2H_2O$ and $Ce(NO_3)_3$•$6H_2O$ by the solvothermal method at 200 °C for 24 h, respectively. The lignin solution was previously prepared by the extraction of wood powder in a mixed solvent of dimethyl sulfoxide (DMSO)/lithium chloride (LiCl). All of the obtained lignin-based carbon/$CePO_4$ nanocomposites were characterized by scanning electron microscopy (SEM), energy-dispersive X-ray spectra (EDS), Fourier transform infrared spectrometry (FT-IR), thermogravimetric analysis (TGA), differential thermal analysis (DTA), and photoluminescence (PL). SEM micrographs showed that the $CePO_4$ concentration had an influence on the size, microstructure, and morphology of the carbon/ $CePO_4$ nanocomposites. The experimental results indicated that the obtained lignin-based carbon/$CePO_4$ nanocomposites had excellent PL properties.

Keywords: Lignin-based carbon; $CePO_4$; Nanocomposites; Solvothermal; Luminescence

*Contact information: a: Beijing Key Laboratory of Lignocellulosic Chemistry, College of Materials Science and Technology, Beijing Forestry University, Beijing 100083, PR China; b: State Key Laboratory of Pulp and Paper Engineering, South China University of Technology, Guangzhou 510640, PR China; *Corresponding author: mg_ma@bjfu.edu.cn*

INTRODUCTION

Since the discovery of carbon nanotubes in 1991 (Iijima 1991), carbon and carbon-based nanocomposites have been receiving more attention due to their unique properties (Baughman *et al.* 2002) such as mechanical properties, high thermal stability, electrical properties, high-temperature and high-pressure stability, resistance to attacks from acids, bases, and solvents, and promising potential applications in electronic conductors (White and Todorov 1998), microelectrodes (Teo *et al.* 2005), field emission transistors (Keren *et al.* 2003), and hydrogen storage (Lin 2000). In addition, carbon and carbon-based nanocomposites can be used for drugs (Bianco *et al.* 2005), proteins, DNA, and catalyst supports (Ruiz-Hitzky *et al.* 2010). Until now, the synthesis of carbon-based nanocomposites made of tellurium/carbon (Qian *et al.* 2006), selenium/carbon (Yu *et al.* 2006), Fe_3O_4/C (Hu and Yu 2006), and $CePO_4$/C (Ma *et al.* 2009) has been successfully carried out.

Polyacrylonitrile has been used as a prominent precursor for carbon materials in the past (Shindo 1961). Lignin is the second most abundant component of biomass in nature after cellulose (Adler 1977). There have been few studies that use cellulose as a precursor for carbonaceous material (Azambrea *et al.* 2000; Ishida *et al.* 2004; Sevilla and Fuertes 2010). Recently, however, lignin was used as a precursor for such carbonaceous materials as activated carbons (Bedia *et al.* 2007; Hayashi *et al.* 2000; Rodríguez-Mirasol *et al.* 1993; Suhas Carrott and Ribeiro Carrott 2007), carbon catalysts (Bedia *et al.* 2009), and carbon-based composite materials (Kosikova *et al.* 1993; Thielemans *et al.* 2002) due to its low cost and high availability. Moreover, lignin is the major component of sulfite pulping black liquor. Thus, lignin can be regarded as a renewable feedstock that is well suited for producing high value-added carbonaceous materials to address environmental problems.

There have also been reports on the fabrication of lignin-based carbon materials. Sudo *et al*. (1992, 1993) reported the process of converting steam-exploded lignin into molten viscous material as a precursor for carbon fibers using the spinning method and the fabrication of carbon fibers from steam-exploded lignin using the phenolysis method based on heat treatment of the molten viscous material under a vacuum. Kubo *et al*. (1998, 2005) reported the use of lignin as a precursor for carbon fibers and investigated the effect of synthetic polymer blending on lignin-based carbon fibers properties. Uraki *et al.* (2001) synthesized activated carbon fibers with large specific surface area from softwood acetic acid lignin. Lallave *et al.* (2007) presented a new, straightforward method for obtaining carbon micro- and nanofibers, both solid and hollow, by co-electrospinning Alcell lignin solutions at room temperature without any added polymer. Microporous active carbon materials with efficient hydrogen electrosorption at ambient conditions have been produced from lignin by standard carbonization and KOH activation at 950 °C (Babel and Jurewicz 2008). Additionally, microporous carbon fibers were synthesized from lignin fibers with and without platinum by electrospinning lignin/ethanol/platinum acetyl acetonate and lignin/ethanol solutions (Ruiz-Rosas *et al.* 2010). Activated carbon with a high capacity for adsorption of metallic ions was prepared by chemical activation of brewer's spent grain lignin using H_3PO_4 at various acid/lignin ratios and carbonization temperatures (Mussatto *et al.* 2010). However, the synthesis of lignin-based carbon/$CePO_4$ nanocomposites using the solvothermal method has not yet been reported.

It is well known that the rare earth phosphates have been extensively used in high performance luminescent devices, sensors, magnets, catalysts, and heat-resistant materials (Feldmann *et al.* 2003). Among these rare earth phosphates, $CePO_4$ can be applied in tribological, heat-resistant, and ceramic materials. In the previous study, $CePO_4$/C core-shell nanorods were synthesized using glucose and $CePO_4$ by the hydrothermal method at 160 °C for 24 h (Ma *et al.* 2009). Additionally, $CePO_4$@$LaPO_4$ one-dimensional nanostructures with highly improved luminescence were fabricated by hydrothermal method (Ma *et al.* 2010).

Herein, the synthesis of lignin-based carbon/$CePO_4$ nanocomposites was reported by the solvothermal method using a lignin solution and $CePO_4$ or NaH_2PO_4•$2H_2O$ and $Ce(NO_3)_3$•$6H_2O$. The solvothermal method is a promising technology for the preparation of inorganic materials. The medium used in the solvothermal process is a non-aqueous

solvent or mixed solvent, which induces the reaction mechanism for the synthesis of inorganic materials caused by the difference in polarity of the organic solvent and water. The lignin solution was previously extracted from wood powder according to a method given in the literature (Wang *et al.* 2009). The solvothermal method provides a high temperature and pressure environment and is favorable for the carbonization of lignin and the fabrication of carbon and $CePO_4$. As one of the most abundant natural phenolic polymers, lignin composes up to one-third of the material found in plant cell walls. In comparison with previous reports (Ma *et al.* 2009), lignin material is cheaper for the synthesis of carbon/$CePO_4$ nanocomposites. Furthermore, it provides a new solution for utilizing renewable resources to alleviate environmental problems and provides new opportunities for high value-added applications of lignin.

EXPERIMENTAL

Methods

Production of lignin solution

All chemicals were of analytical grade and used as received without further purification. All experiments were conducted under an air atmosphere. The lignin solution was extracted from wood powder as previously described (Ruiz-Rosas *et al.* 2010). In a typical synthesis, 3.000 g wood powder and 1.200 g LiCl were added to 30 mL of dimethyl sulfoxide (DMSO) under vigorous stirring at room temperature for 1 h. Then, the obtained solution was heated to 140 °C for 1 h by microwave heating. After that, the mixture was precipitated by 95% ethanol. The obtained precipitate was made of cellulose and hemicellulose. The filtrate was heated in a water bath and concentrated by a rotary evaporator at 50 °C. Finally, the lignin solution was obtained in a mixed solvent of DMSO/ethanol.

Fabrication of $CePO_4$

The synthesis of $CePO_4$ was carried out as follows: 0.156 g $NaH_2PO_4 \cdot 2H_2O$ and 0.434 g $Ce(NO_3)_3 \cdot 6H_2O$ were added into 15 mL of distilled water under vigorous stirring for 30 min. The obtained solution was hydrothermally treated at 200 °C for 24 h without stirring or shaking, and was then allowed to naturally cool down to room temperature. Subsequently, the remaining $CePO_4$ precipitate was used for the preparation of lignin-based carbon/$CePO_4$ nanocomposites.

Preparation of lignin-based carbon/$CePO_4$ nanocomposites

For the synthesis of lignin-based carbon/$CePO_4$ nanocomposites, $CePO_4$ precipitate was highly dispersed in 30 mL of the obtained lignin solution. The resulting suspension was poured into a Teflon-lined autoclave. The autoclave was sealed, maintained at 200 °C for 24 h, and then air-cooled to room temperature. The resulting precipitate was separated from the solution by centrifugation, washed by ethanol several times, and dried at 60 °C for further characterization. These samples were denoted sample 1, 2, and 3. The experimental parameters for the synthesis of the samples are listed in Table 1.

Table 1. Detailed Experimental Parameters for the Synthesis of Samples Prepared by the Solvothermal Method at 200 °C for 24 h

Sample	Reaction system
1	One-third of precipitate $CePO_4$* + 30 mL lignin solution
2	Half of precipitate $CePO_4$* + 30 mL lignin solution
3	The whole precipitate $CePO_4$* + 30 mL lignin solution
4	0.078 g $NaH_2PO_4 \cdot 2H_2O$ + 0.217 g $Ce(NO_3)_3 \cdot 6H_2O$ + 30 mL lignin solution
5	0.156 g $NaH_2PO_4 \cdot 2H_2O$ + 0.434 g $Ce(NO_3)_3 \cdot 6H_2O$ + 30 mL lignin solution
6	0.312 g $NaH_2PO_4 \cdot 2H_2O$ + 0.868 g $Ce(NO_3)_3 \cdot 6H_2O$ + 30 mL lignin solution

*The precipitate $CePO_4$ was obtained using 0.156 g $NaH_2PO_4 \cdot 2H_2O$ and 0.434 g $Ce(NO_3)_3 \cdot 6H_2O$ by the hydrothermal method at 200 °C for 24 h.

For comparison, lignin-based carbon/$CePO_4$ nanocomposites were also synthesized as follows: $NaH_2PO_4 \cdot 2H_2O$ and $Ce(NO_3)_3 \cdot 6H_2O$ were added directly into the obtained lignin solution (30 mL) under vigorous magnetic stirring. The resulting suspension was poured into a Teflon-lined autoclave. The autoclave was sealed, maintained at 200 °C for 24 h, and then air-cooled to room temperature. The resulting precipitate was separated from the solution by centrifugation, washed with ethanol several times, and dried at 60 °C for further characterization. The samples were denoted sample 4, 5, and 6, as shown in Table 1.

Characterization

Scanning electron microscopy (SEM) images were recorded with a Hitachi 3400 N scanning electron microscope. All samples were coated with a layer of Au about 20 nm thick prior to examination by SEM. The energy-dispersive X-ray spectra (EDS) attached to the scanning electron microscopy were used to analyze the composition of the sample. X-ray powder diffraction (XRD) patterns were recorded in 2θ range from 10° to 70° on an X'Pert PRO MPD diffractometer operating at 40 kV with Cu Kα (λ = 1.5405Å) radiation. Fourier transform infrared (FT-IR) spectroscopy was carried out on an FT-IR spectrophotometer (Nicolet 510) using the KBr disk method. The thermal behavior of the samples was tested using thermogravimetric analysis (TGA) and differential thermal analysis (DTA) on a simultaneous thermal analyzer (DTG-60, Shimadzu) at a heating rate of 10 °C min^{-1} in flowing air. Photoluminescence (PL) spectra were obtained using a fluorescence spectrophotometer (Perkin-Elmer LS-55) with a xenon lamp as the excitation source with an excitation wavelength of 280 nm.

RESULTS AND DISCUSSION

The morphology and microstructures of the lignin-based carbon/$CePO_4$ nanocomposites, which were synthesized by the solvothermal method using one-third, half,

and the entire $CePO_4$ precipitate together with the lignin solution at 200 °C for 24 h, were investigated by SEM, as shown in Fig. 1. When one-third of the $CePO_4$ precipitate was used with the lignin to fabricate carbon/$CePO_4$ nanocomposites, spheres and congregated fiber-like shapes were observed (Fig. 1a). A magnified micrograph of the sphere-like morphology is shown in Fig. 1b. The spheres had diameters of about 4.5 μm and most nanoparticles were bound to the sphere surface. Compared with Fig. 1a and 1b, there was no significant difference in the morphology of the nanocomposites made using half of the $CePO_4$ precipitate (Fig. 1c). A magnified micrograph of the sphere-like morphology is shown in Fig. 1d. The spheres had diameters of about 4.1 μm, and some nanoparticles were also bound to the sphere surface. Increasing the $CePO_4$ concentration from half to the whole $CePO_4$ precipitate resulted in similar morphology (Fig. 1e). A magnified micrograph of the sphere-like morphology is shown in Fig. 1f. The spheres had diameters of about 3.6 μm, and almost no nanoparticles were observed on the sphere surface. The size of the spheres decreased and the sphere surface became smooth with increasing $CePO_4$ concentration, indicating that the $CePO_4$ concentration had an influence on the size and microstructure of lignin-based carbon/$CePO_4$ nanocomposites.

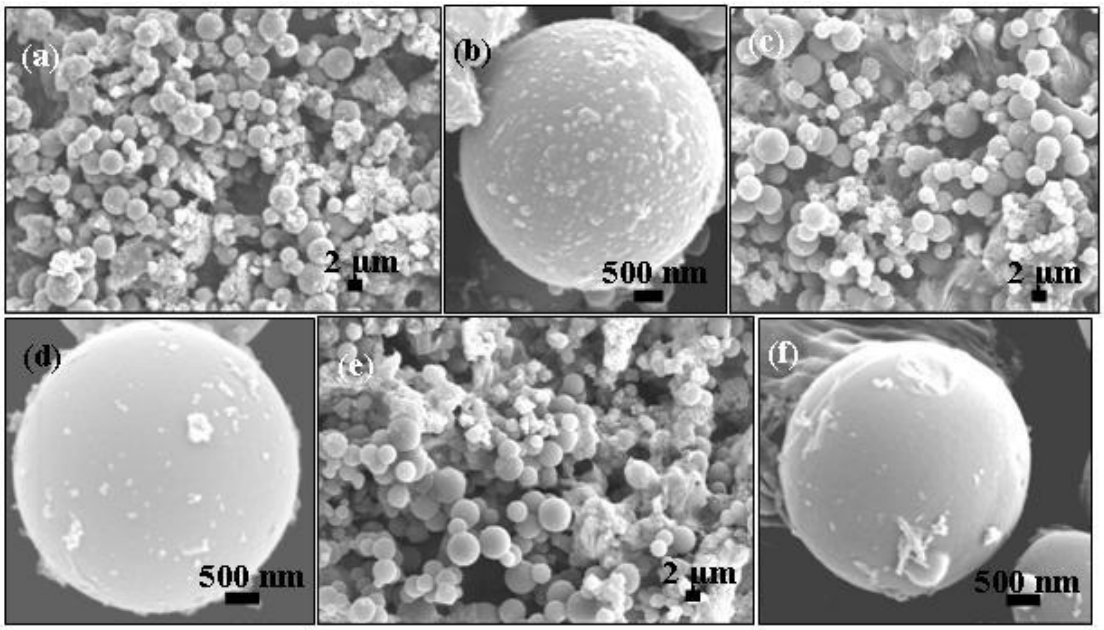

Fig. 1. SEM micrographs of the lignin-based carbon/$CePO_4$ nanocomposites synthesized by the solvothermal method using different $CePO_4$ precipitate at 200 °C for 24 h: sample 1 (a, b); sample 2 (c, d); sample 3 (e, f)

Lignin-based carbon/$CePO_4$ nanocomposites were also synthesized by the solvothermal method using lignin solution, NaH_2PO_4•$2H_2O$, and $Ce(NO_3)_3$•$6H_2O$ at 200 °C for 24 h. When 0.078 g NaH_2PO_4•$2H_2O$ and 0.217 g $Ce(NO_3)_3$•$6H_2O$ were used for the preparation of carbon/$CePO_4$ nanocomposites, sphere-like and rose-like morphologies consisting of curved nanosheet building blocks were obtained, as shown in Fig. 2a-c. Magnified micrographs of the sphere-like and rose-like morphologies are shown in Fig. 2b and c, respectively. The nanoparticles were bound to the sphere surface, so the sphere was not stable under electron beam irradiation and surface bulging was observed (Fig.

2b). When the NaH_2PO_4•$2H_2O$ and $Ce(NO_3)_3$•$6H_2O$ concentrations were increased to 0.156 g and 0.434 g, sphere-like and carnation-like morphologies were also observed (Fig. 2d-f). Individual carnation-like shapes are shown in Fig. 2e and f. In addition, a few single sheets were also observed. When the NaH_2PO_4•$2H_2O$ and $Ce(NO_3)_3$•$6H_2O$ concentrations were increased to 0.312 g and 0.868 g, sphere-like shapes were observed as the major morphology, while nanosheets and rose-like shapes were observed as minor morphologies (Fig. 2g-i). Figures 2h and i show the detailed structure of the sphere-like morphology, which had diameters of about 4.66 μm and consisted of curved nanosheet building blocks. Different morphologies were observed from different NaH_2PO_4•$2H_2O$ and $Ce(NO_3)_3$•$6H_2O$ concentrations, indicating that concentrations of NaH_2PO_4•$2H_2O$ and $Ce(NO_3)_3$•$6H_2O$ played an important role in the shape and microstructure of lignin-based carbon/$CePO_4$ nanocomposites. Moreover, the shapes of nanocomposites in Fig. 2 were different from those shown in Fig. 1.

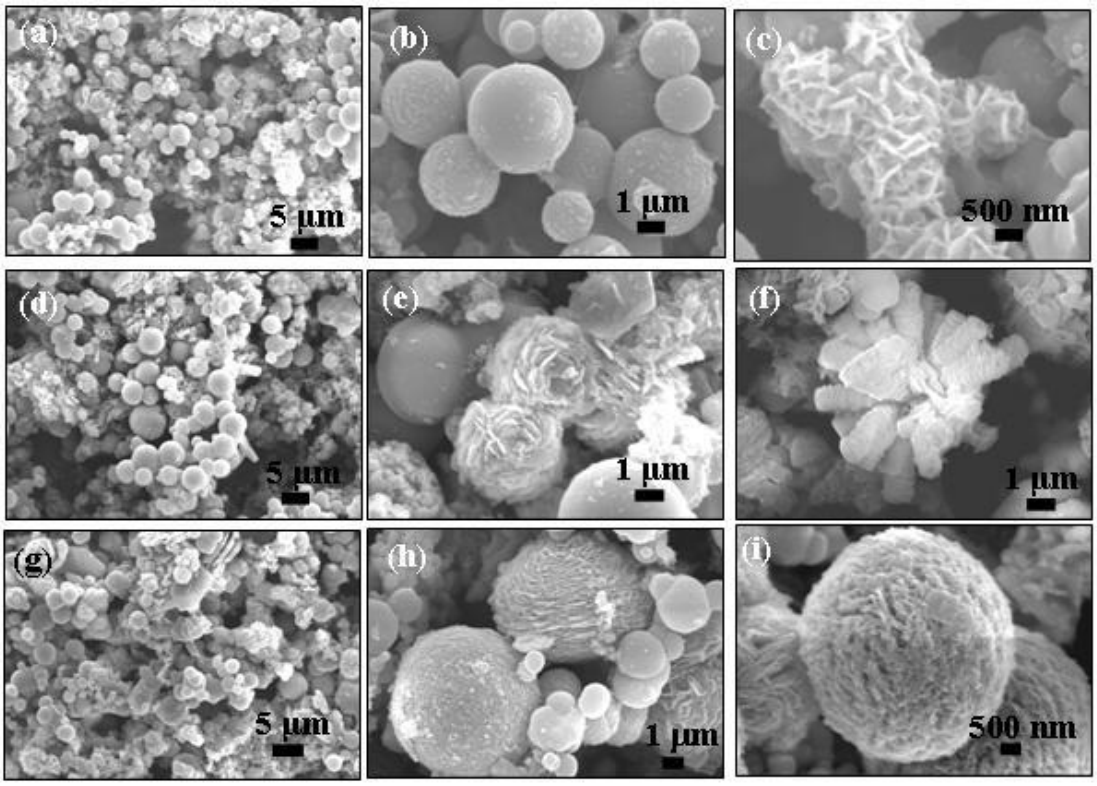

Fig. 2. SEM micrographs of the lignin-based carbon/$CePO_4$ nanocomposites synthesized by the solvothermal method using different NaH_2PO_4•$2H_2O$ and $Ce(NO_3)_3$•$6H_2O$ concentrations at 200 °C for 24 h: sample 4 (a-c); sample 5 (d-f); sample 6 (g-i)

To further observe the morphology and microstructure of the lignin-based carbon/$CePO_4$ nanocomposites, the samples were investigated by TEM, as shown in Fig. S1. When half of the $CePO_4$ precipitate was used to fabricate carbon/$CePO_4$ nanocomposites, $CePO_4$ nanorods had relatively uniform sizes with diameters ranging from 25 to 35 nm and lengths of up to several micrometers (Fig. S1a-c). When the NaH_2PO_4•$2H_2O$ and $Ce(NO_3)_3$•$6H_2O$ concentrations were increased to 0.156 g and 0.434 g, nanoparticles and curved nanosheet building blocks were clearly observed (Fig. S1d-f). Finally, when

NaH_2PO_4•$2H_2O$ and $Ce(NO_3)_3$•$6H_2O$ concentrations were increased to 0.312 g and 0.868 g, nanosheets and nanoparticles were obtained (Fig. S1g-i). SEM and TEM results confirmed the synthesis of lignin-based carbon/$CePO_4$ nanocomposites.

In a previous study, $CePO_4$/C core-shell nanorods were obtained using glucose as the carbon source by the hydrothermal method (Ma *et al.* 2009). However, in this work, sphere-like, congregated fiber-like, flower-like, and carnation-like shapes were observed using lignin as the carbon source, as shown in Fig. 1 and 2. Glucose is a monosaccharide, which is easily carbonized to fabricate core-shell nanorods using $CePO_4$ nanorods as a template. Lignin is a complex polyphenolic amorphous polymer originating from the copolymerization of three phenylpropanoid monomers, *i.e.*, coniferyl, sinapyl, and pcoumaryl alcohol. Therefore, the carbonization of lignin is a more complex process. Furthermore, the mixed solvents of DMSO/ethanol were used under solvothermal conditions. The different solvents had different adsorption ability on various facets, leading to the different growth rates for different crystal facets of lignin-based carbon/ $CePO_4$ nanocomposites. Of course, the intrinsic reasons for the morphological changes of the lignin-based carbon/$CePO_4$ nanocomposites still need to be investigated further.

Figure S2a shows the EDS spectrum of the sample synthesized by the solvothermal method using lignin solution, 0.312 g of NaH_2PO_4•$2H_2O$, and 0.868 g of $Ce(NO_3)_3$•$6H_2O$ at 200 °C for 24 h. The sample consisted of C, O, Ce, and P, the right composition of lignin-based carbon/$CePO_4$ nanocomposites. The Cu signal came from the SEM copper grid of the sample holder. The Au signal came from the Au coated to a thickness of about 20 nm prior to examination by SEM. Figures S2b-e show the EDS elemental mapping images of C, O, Ce, and P, respectively, which further confirmed the correct composition of the lignin-based carbon/$CePO_4$ nanocomposites. The EDS elemental mapping image of C in Fig. S2b also indicated the existence of carbon spheres. The EDS elemental mapping images of O, Ce, and P in Fig. S2c-e implied homogeneous distribution of $CePO_4$.

The $CePO_4$ phase of the lignin-based carbon/$CePO_4$ nanocomposites was characterized with XRD, as shown in Fig. S3. All of the samples had similar XRD patterns, which can be readily indexed to the $CePO_4$ with a monoclinic structure (JCPDS 32-0199). The pattern peak intensity (Fig. S3d-f) of the samples synthesized by mixing the lignin solution, NaH_2PO_4•$2H_2O$, and $Ce(NO_3)_3$•$6H_2O$ was stronger than that of the samples synthesized by mixing lignin and $CePO_4$ (Fig. S3a-c). Simultaneous formation of carbon from the lignin solution and $CePO_4$ nanoparticles led to homogeneity within the composite structures of carbon and $CePO_4$ nanoparticles. When the concentration of NaH_2PO_4•$2H_2O$ and $Ce(NO_3)_3$•$6H_2O$ increased, a peak from impurity was observed at $2\theta = 16.1^o$ (Fig. S3e,f). No peaks from carbon were observed in any of the XRD patterns. The XRD results confirmed that the obtained carbon was amorphous. The sizes of $CePO_4$ nanostructures were calculated according to the Scherrer formula,

$$D = K\lambda / (\beta \cos \theta) \quad (1)$$

where K is a constant, λ is 1.5405 Å, and β is half peak width. Here, K is assigned as 1. The sizes of samples 1 through 6 were 37 nm, 36 nm, 34 nm, 33 nm, 42 nm, and 41 nm, respectively.

The lignin-based carbon/$CePO_4$ nanocomposites were further examined by FT-IR analysis, as shown in Fig. S4. All samples exhibited the characteristic absorptions of lignin and $CePO_4$. The band at ~3480 cm^{-1} is attributed to O-H stretching vibration. The bands at ~2970 and 2918 cm^{-1} are due to the C-H stretching of aliphatic and aromatic carbons. The band at ~1616 cm^{-1} is indicative of the C=O stretching of carbonyls (Friese and Banerjee 1992). The shoulder at 1711 cm^{-1} is assigned to unconjugated carbonyls. The bands due to the asymmetric stretching of PO_3 terminal groups from pyrophosphate were observed at ~1201 and 1104 cm^{-1}. The band at ~948 cm^{-1} is characteristic of the symmetric stretching vibrations of PO_3 groups, while the absorption bands at ~643 cm^{-1} and in the region of 400 to 600 cm^{-1} belong to the O=P-O bending and O-P-O bending modes of the deformation of PO_2 and PO_3 groups. The similar spectral profiles indicated the similar structures of the cellulose in composites. However, compared to the samples synthesized by the solvothermal method using lignin solution and $CePO_4$ (Fig. S4a-c), the intensity of the peak at 948 cm^{-1} decreased for the samples prepared using lignin, $NaH_2PO_4 \cdot 2H_2O$, and $Ce(NO_3)_3 \cdot 6H_2O$ (Fig. S4d-f). This result indicated the decreasing of PO_3 groups, which was due to the relatively homogenous composition of $CePO_4$ and carbon. We investigated the structure of lignin-based carbon/$CePO_4$ nanocomposites by the cross polarization magic angle spinning (CP/MAS) ^{13}C-NMR spectrum (data not given). Unfortunately, no noticeable signals were observed in the ^{13}C-NMR spectrum. Only three broad weak peaks were obtained in the regions of 0 to 20 ppm, 100 to 150 ppm, and 160 to 200 ppm. The intrinsic reason needs to be further explored in the near future. Raman spectra were also applied to characterize the structure of lignin-based carbon/$CePO_4$ nanocomposites (data not given). Only a weak peak was observed at 1521 cm^{-1}, assigning to the carbon. No other peaks were obtained.

The thermal stability of the lignin-based carbon/$CePO_4$ nanocomposites is very important for their application, so it was also investigated by TGA and DTA. The TGA and DTA curves for the prepared nanocomposites are shown in Figs. S5 and S6. The TGA curves of the lignin-based carbon/$CePO_4$ nanocomposites synthesized by mixing the lignin solution and $CePO_4$ exhibited a small weight loss at about 150 °C due to the loss of adsorbed water molecules that came from the ambient environment (Fig. S5A). This weight loss was accompanied by endothermic peaks at about 150 °C in the DTA curves (Fig. S5B). The obvious weight losses of the lignin-based carbon/$CePO_4$ nanocomposites were ~37.8 %, 33.0%, and 23.4% from 250 °C to 600 °C in the TGA curves for samples 1, 2, and 3 (Fig. S5A), indicating that the weight losses decreased with increasing $CePO_4$ concentration. The weight loss was attributable to the thermal decomposition of carbon in the composites and degradation of the carbohydrate components of lignin, which were degraded to volatile gases including CO, CO_2, and CH_4. The corresponding endothermic peaks were observed at about 579 °C in the DTA curves (Fig. S5B). For comparison, the TGA and DTA curves of the samples synthesized by mixing lignin, $NaH_2PO_4 \cdot 2H_2O$, and $Ce(NO_3)_3 \cdot 6H_2O$ are also shown in Fig. S6. The weight losses were ~34.8 %, 28.5%, and 36.7% from 250 °C to 600 °C in the TGA curves (Fig. S6A), which was not in agreement with the results shown in Fig. S5A. The DTA curves of the samples synthesized using 0.078 g $NaH_2PO_4 \cdot 2H_2O$ and 0.217 g $Ce(NO_3)_3 \cdot 6H_2O$, 0.156 g $NaH_2PO_4 \cdot 2H_2O$, and 0.434 g $Ce(NO_3)_3 \cdot 6H_2O$ showed endothermic peaks at about 106 °C and 129 °C, respectively (Fig. S6B). However, the DTA curve of the

sample synthesized using 0.312 g NaH_2PO_4•$2H_2O$ and 0.868 g $Ce(NO_3)_3$•$6H_2O$ did not show a peak in this temperature region. Moreover, an endothermic peak at about 262 °C was observed in all of the DTA curves. Based on the TGA results from Fig. S5 and S6, the $CePO_4$ concentrations were ~62.2%, 67.0%, 76.6%, 65.2%, 71.5%, and 63.3% for samples 1 through 6. Samples 1 to 3 were synthesized using one-third, half, and whole of precipitate $CePO_4$, inducing the increasing $CePO_4$ concentrations in the lignin-based carbon/$CePO_4$ nanocomposites. However, samples 4 to 6 were synthesized using 0.078 g NaH_2PO_4•$2H_2O$ and 0.217 g $Ce(NO_3)_3$•$6H_2O$, 0.156 g NaH_2PO_4•$2H_2O$ and 0.434 g $Ce(NO_3)_3$•$6H_2O$, and 0.312 g NaH_2PO_4•$2H_2O$ and 0.868 g $Ce(NO_3)_3$•$6H_2O$. The concentration of $Ce(NO_3)_3$ and NaH_2PO_4•$2H_2O$ increased relative to the lignin in samples 4 through 6. As is well known, it is difficult to obtain a 100% conversion rate of $CePO_4$ from $Ce(NO_3)_3$ and NaH_2PO_4•$2H_2O$ in nanocomposites. Therefore, the concentration of $CePO_4$ in nanocomposites was not in accordance with the concentration of $Ce(NO_3)_3$ and NaH_2PO_4•$2H_2O$. The $CePO_4$ concentrations did not increase with increasing concentrations of NaH_2PO_4•$2H_2O$ and $Ce(NO_3)_3$•$6H_2O$.

Luminescent spectra of the lignin-based carbon/$CePO_4$ nanocomposites with an excitation wavelength of 280 nm were also obtained, as shown in Fig. 3. Figures 3a-c show the PL spectra of the nanocomposites synthesized by mixing lignin and $CePO_4$. There is a weak peak in the visible region around 467 nm and a strong emission peak centered at 318 nm, which may be ascribed to the d-f transitions of Ce^{3+} ions (Bu *et al.* 2004). The peak intensity of the lignin-based carbon/$CePO_4$ nanocomposites increased with increasing $CePO_4$ concentration, indicating improved luminescent efficiency. Therefore, the peak intensity of nanocomposites can be adjusted by changing the $CePO_4$ concentration. However, two strong emission peaks centered in the 310 to 340 nm region were observed in a previous study on $CePO_4$@C and $CePO_4$@$LaPO_4$ composites (Ma *et al.* 2009, 2010). The PL spectra of the lignin-based carbon/$CePO_4$ composites synthesized by mixing the lignin, NaH_2PO_4•$2H_2O$, and $Ce(NO_3)_3$•$6H_2O$ are shown in Fig. 3d-f. The strong emission peak of lignin-based carbon/$CePO_4$ nanocomposites in Fig. 3d-f was centered at a similar wavelength (321 nm) to Fig. 3a-c. Moreover, the peak intensity of lignin-based carbon/$CePO_4$ nanocomposites also increased with increasing $CePO_4$ concentration. These results indicated the successful synthesis of lignin-based carbon/$CePO_4$ nanocomposites with good PL properties. Moreover, the peak intensities of lignin-based carbon/$CePO_4$ nanocomposites were much weaker than previous results (Ma *et al.* 2009, 2010).

Factors such as the concentration, size, shape, microstructures, and dispersion of nanocomposites might have an effect on the peak intensity of PL spectra. In this work, the $CePO_4$ concentrations were between 62.2% and 76.6% for samples 1 through 6. The percentage of lignin-based carbon in nanocomposites was between 23.4% and 37.8%, inducing the low peak intensity of PL spectra. Moreover, as indicated by Bu *et al.* (2005), a significant amount of nonradiative centers existed on the surface of $CePO_4$ nanowires, which absorbed the energy of the electron and gave no light emissions. While $CePO_4$/C core-shell nanorods and $CePO_4$@$LaPO_4$ one-dimensional nanostructures with good dispersion were obtained in previous works (Ma *et al.* 2009, 2010), lignin-based carbon/$CePO_4$ nanocomposites with different morphologies (sphere, congregated fiber-like, flower, and carnation) were observed in this work. The $CePO_4$ was not formed as a

composite with lignin-based carbon to fabricate core-shell structure, which may help to explain the difference in PL property, compared with the previous reports (Ma *et al.* 2009, 2010).

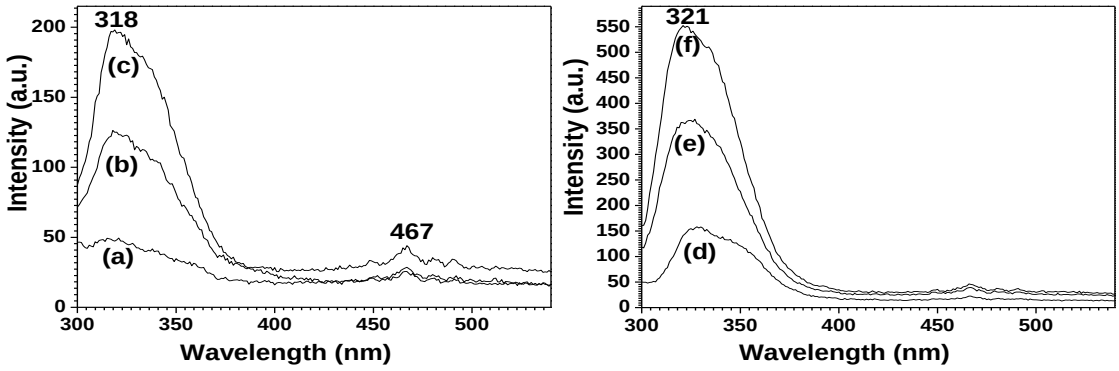

Fig. 3. PL spectra of the lignin-based carbon/$CePO_4$ nanocomposites (λexc = 280 nm): sample 1 (a); sample 2 (b); sample 3 (c); sample 4 (d); sample 5 (e); sample 6 (f)

CONCLUSIONS

1. The synthesis of the lignin-based carbon/$CePO_4$ nanocomposites was reported using a hydrothermal method and mixing the lignin solution with $CePO_4$ or NaH_2PO_4•$2H_2O$ and $Ce(NO_3)_3$•$6H_2O$.
2. SEM micrographs indicated that the $CePO_4$ concentration had an influence on the size and microstructure of carbon/$CePO_4$ nanocomposites, while the NaH_2PO_4•$2H_2O$ and $Ce(NO_3)_3$•$6H_2O$ concentrations also played an important role in the shape and microstructure of carbon/$CePO_4$ nanocomposites.
3. The PL spectra of the carbon/$CePO_4$ nanocomposites showed that the peak intensity of nanocomposites can be adjusted by changing the $CePO_4$ concentration.
4. The synthetic strategy reported in this work provides a new opportunity for high value-added applications of lignin. The lignin-based carbon/$CePO_4$ nanocomposites might be a very promising candidate for the application in luminescent devices.

ACKNOWLEDGMENTS

Financial support from the Fundamental Research Funds for the Central Universities (No. TD2011-11, JC2013-3), Beijing Nova Program (Z121103002512030), the Program for New Century Excellent Talents in University (NCET-11-0586), National Natural Science Foundation of China (31070511), and Research Fund for the Doctoral Program of Higher Education of China (20100014120010) is gratefully acknowledged.

REFERENCES CITED

Adler, E. (1977). "Lignin chemistry- Past, present and future," *Wood Sci. Technol.* 11(3), 169-218.

Azambrea, B., Heintza, O., Krztonb, A., Zawadzkic, J., and Weber, J. V. (2000). "Cellulose as a precursor of catalyst support: New aspects of thermolysis and oxidation - IR, XPS and TGA studies," *J. Analyt. Appl. Pyrolys.* 55(1), 105-117.

Babel, K., and Jurewicz, K. (2008). "KOH activated lignin based nanostructured carbon exhibiting high hydrogen electrosorption," *Carbon* 46(14), 1948-1956.

Baughman, R. H., Zakhidov, A. A., and de Heer, W. A. (2002). "Carbon nanotubes- The route toward applications," *Science* 297(5582), 787-792.

Bedia, J., Rodríguez-Mirasol, J., and Cordero, T. (2007). "Water vapour adsorption on lignin-based activated carbons," *J. Chem. Technol. Biotechnol.* 82(6), 548-557.

Bedia, J., Rosas, J. M., Márquez, J., Rodríguez-Mirasol, J., and Cordero, T. (2009). "Preparation and characterization of carbon based acid catalysts for the dehydration of 2-propanol," *Carbon*, 47, 286-294.

Bianco, A., Kostarelos, K., and Prato, M. (2005). "Applications of carbon nanotubes in drug delivery," *Current Opinion in Chemical Biology* 9(6), 674-679.

Bu, W. B., Chen, H., Hua, Z. L., Liu, Z., Zhang, L., and Shi, J. L. (2004). "Surfactant-assisted synthesis of Tb(III)-doped cerium phosphate single-crystalline nanorods with enhanced green emission," *Appl. Phys. Lett.* 85(19), 4307-4309.

Bu, W. B., Hua, Z. L., Chen, H., and Shi, J. L. (2005). "Epitaxial synthesis of uniform cerium phosphate one-dimensional nanocable heterostructures with improved luminescence," *J. Phys. Chem. B* 109(30), 14461-14464.

Feldmann, C., Jüstel, T., Ronda, C. R., and Schmidt, P. J. (2003). "Inorganic luminescent materials-100 years of research and application," *Adv. Funct. Mater.* 13(7), 511-516.

Friese, M. A., and Banerjee, S. (1992). "Lignin determination by FT-IR," *Appl. Spectrosc.* 46(2), 246-248.

Hayashi, J., Kazehaya, A., Muroyama, K., and Watkinson, A. P. (2000). "Preparation of activated carbon from lignin by chemical activation," *Carbon* 38(13), 1873-1878.

Hu, X. L., and Yu, J. C. (2006). "Microwave-assisted synthesis of a superparamagnetic surface-functionalized porous Fe_3O_4/C," *Chem. Asian J.* 1(4), 605-610.

Iijima, S. (1991). "Helical microtubules of graphitic carbon," *Nature* 354, 56-58.

Ishida, O., Kim, D. Y., Kuga, S., Nishiyama, Y., and Brown, R. M. (2004). "Microfibrillar carbon from native cellulose," *Cellulose* 11, 475-480.

Keren, K., Berman, R. S., Buchstab, E., Sivan, U., and Braun, E. (2003). "DNA-templated carbon nanotube field-effect transistor," *Science* 302(5649), 1380-1382.

Kosikova, B., Demianova, V., and Kacurakova, M. (1993). "Sulfur-free lignins as composites of polypropylene films," *J. Appl. Polym. Sci.* 47(6), 1065-1074.

Kubo, S., and Kadla, J. F. (2005). "Lignin-based carbon fibers: Effect of synthetic polymer blending on fiber properties," *J. Polym. Environment* 13(2), 97-105.

Kubo, S., Uraki, Y., and Sano, Y. (1998). "Preparation of carbon fibers from softwood lignin by atmospheric acetic acid," *Carbon* 36(7-8), 1119-1124.

Lallave, M., Bedia, J., Ruiz-Rosas, R., Rodríguez-Mirasol, J., Cordero, T., Otero, J. C., Marquez, M., Barrero, A., and Loscertales, I. G. (2007). "Filled and hollow carbon nanofibers by coaxial electrospinning of Alcell lignin without binder polymers," *Adv. Mater.* 19(23), 4292-4296.

Lin, J. Y. (2000). "Hydrogen storage in nanotubes," *Science* 287(5460), 1929.

Ma, M. G., Zhu, J. F., Cao, S. W., Chen, F., and Sun, R. C. (2010). "Hydrothermal synthesis of relatively uniform $CePO_4$@$LaPO_4$ one-dimensional nanostructures with highly improved luminescence," *J. All. Comp.* 492(1-2), 559-563.

Ma, M. G., Zhu, J. F., Sun, R. C., and Zhu, Y. J. (2009). "Hydrothermal synthesis and characterization of $CePO_4$/C core-shell nanorods," *Mater. Lett.* 63(28), 2513-2515.

Mussatto, S. I., Fernandes, M., Rocha, G. J. M., Orfao, J. J. M., Teixeira, J. A., and Roberto, I. C. (2010). "Production, characterization and application of activated carbon from brewer's spent grain lignin," *Bioresour. Technol.* 101(7), 2450-2457.

Qian, H. S., Yu, S. H., Luo, L. B., Gong, J. Y., Fei, L. F., and Liu, X. M. (2006). "Synthesis of uniform Te@carbon rich composite nanocables with photoluminescent property and carbonaceous nanofibers by hydrothermal carbonization of glucose," *Chem. Mater.* 18(8), 2102-2108.

Rodríguez-Mirasol, J., Cordero, T., and Rodríguez, J. J. (1993). "Activated carbons from CO_2 partial gasification of eucalyptus kraft lignin," *Energy Fuels* 7(1), 133-138.

Ruiz-Hitzky, E., Darder, M., Aranda, P., and Ariga, K. (2010), "Advances in biomimetic and nanostructured biohybrid materials," *Adv. Mater.* 22(3), 323-336**.**

Ruiz-Rosas, R., Bedia, J., Lallave, M., Loscertales, I. G., Barrero, A., Rodríguez-Mirasol, J., and Cordero, T. (2010). "The production of submicron diameter carbon fibers by the electrospinning of lignin," *Carbon* 48(3), 696-705.

Sevilla, M., and Fuertes, A. B. (2010). "Graphitic carbon nanostructures from cellulose," *Chem. Phys. Lett.* 490(1-3), 63-68.

Shindo, A. (1961). "Research report of Osaka Industrial Institute," 12, 110-116.

Sudo, K., and Shlmlzu, K. (1992). "A new carbon fiber from lignin," *J. Appl. Polym. Sci.* 44(1), 127-134.

Sudo, K., Shlmlzu, K., Nakashima, N., and Yokoyama, A. (1993). "A new modification method of exploded lignin for the preparation of a carbon fiber precursor," *J. Appl. Polym. Sci.* 48(8), 1485-1491.

Suhas Carrott, P. J. M., and Ribeiro Carrott, M. M. L. (2007). "Lignin-from natural adsorbent to activated carbon: A review," *Bioresour. Technol.* 98(12), 2301-2312.

Teo, K. B. K., Minoux, E., Hudanski, L., Peauger, F., Schnell, J. P., Gangloff, L., Legagneux, P., Dieumegard, D., Amaratunga, G. A. J., and Milne, W. I. (2005). "Microwave devices- Carbon nanotubes as cold cathodes," *Nature* 437, 968.

Thielemans, W., Can, E., Morye, S. S., and Wool, R. P. (2002). "Novel applications of lignin in composite materials," *J. Appl. Polym. Sci.* 83(2), 323-331.

Uraki, Y., Nakatani, A., Kubo, S., and Sano, Y. (2001). "Preparation of activated carbon fibers with large specific surface area from softwood acetic acid lignin," *J. Wood Sci.* 47(6), 465-469.

Wang, Z. G., Yokoyama, T., Chang, H. M., and Matsumoto, Y. (2009). "Dissolution of beech and spruce milled woods in LiCl/DMSO," *J. Agr. Food Chem.* 57(14), 6167-6170.

White, C. T., and Todorov, T. N. (1998). "Carbon nanotubes as long ballistic conductors," *Nature* 393 240-242.

Yu, J. C., Hu, X. L., Li, Q., Zheng, Z., and Xu, Y. M. (2006). "Synthesis and characterization of core-shell selenium/carbon colloids and hollow carbon capsules," *Chem. Eur. J.* 12(2), 548-552.

Article submitted: March 10, 2013; Peer review completed: May 21, 2013; Revised version received: June 14, 2013; Accepted: June 16, 2013; Published: June 19, 2013.

APPENDIX

Supplemental Figures

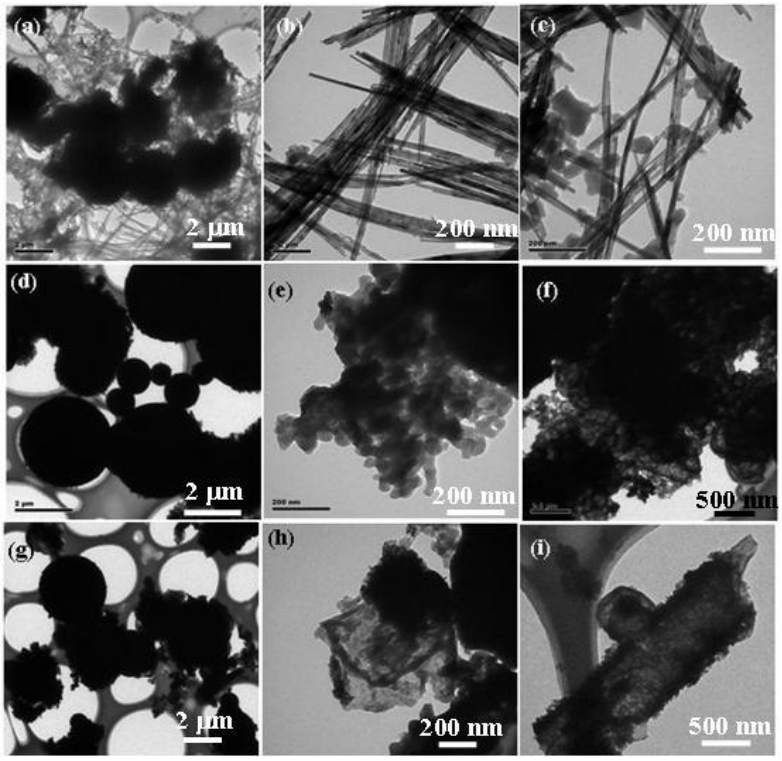

Fig. S1. TEM micrographs of the lignin-based carbon/$CePO_4$ nanocomposites: (a-c) sample 2; (d-f) sample 5; (g-i) sample 6.

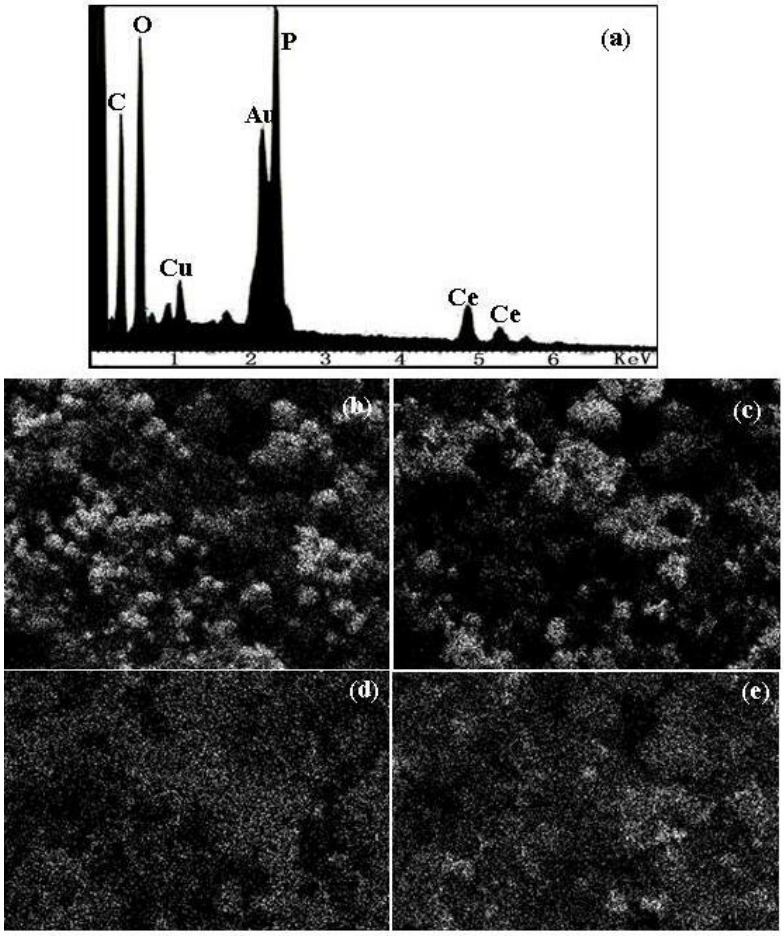

Fig. S2. (a) EDS spectrum, (b-e) the EDS elemental mapping images of the lignin-based carbon/$CePO_4$ nanocomposites (sample 6): (b) C; (c) O; (d) Ce; and (e) P.

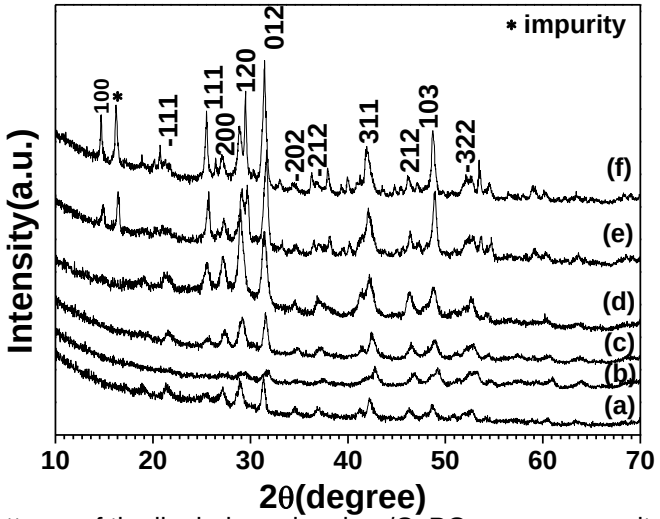

Fig. S3. XRD patterns of the lignin-based carbon/$CePO_4$ nanocomposites: (a) sample 1; (b) sample 2; (c) sample 3; (d) sample 4; (e) sample 5; (f) sample 6.

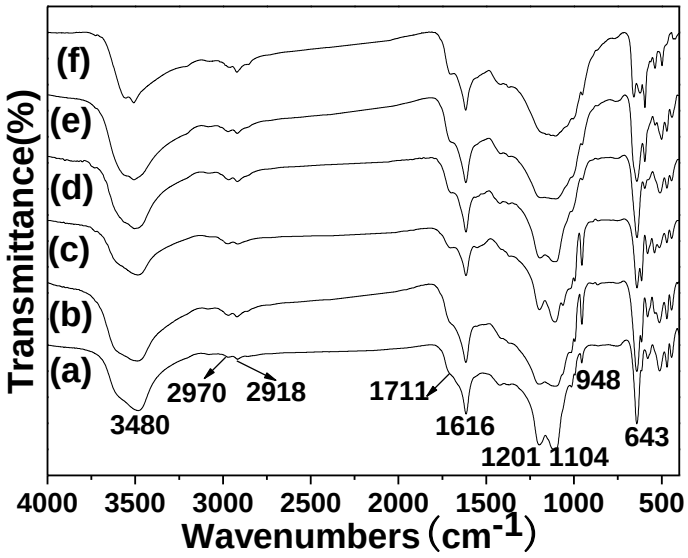

Fig. S4. FT-IR spectra of the lignin-based carbon/$CePO_4$ nanocomposites: (a) sample 1; (b) sample 2; (c) sample 3; (d) sample 4; (e) sample 5; (f) sample 6

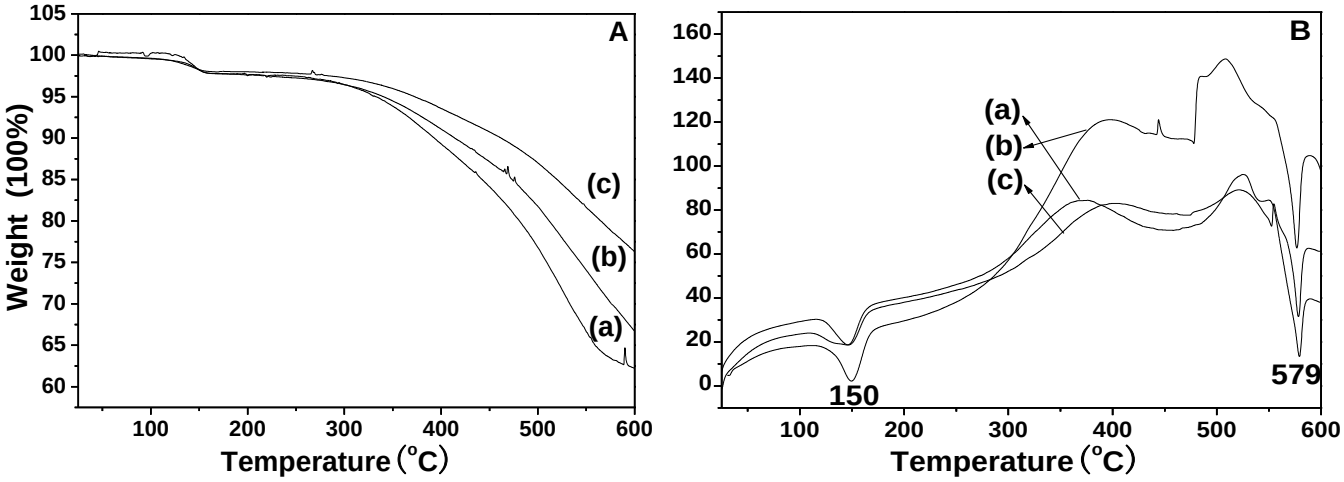

Fig. S5. (A) TGA and (B) DTA curves of the lignin-based carbon/$CePO_4$ nanocomposites: (a) sample 1; (b) sample 2; (c) sample 3

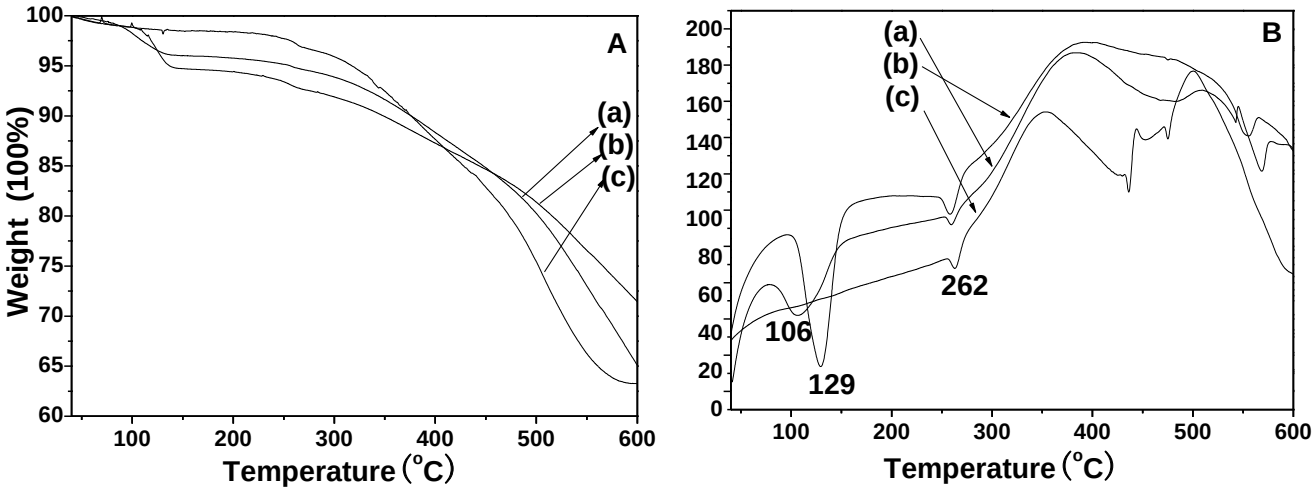

Fig. S6 (A) TGA and (B) DTA curves of the lignin-based carbon/$CePO_4$ nanocomposites: (a) sample 4; (b) sample 5; (c) sample 6